Pergamon

0956-7151(95)00385-1

Acta mater. Vol. 44, No. 7, pp. 2797–2807, 1996

Published by Elsevier Science Ltd

1359-6454/96 $15.00 + 0.00

DYNAMIC BAUSCHINGER EFFECT

A. THAKUR, S. NEMAT-NASSER and K. S. VECCHIO

Center for Excellence for Advanced Materials, Department of Applied Mechanics and Engineering Sciences, University of California, San Diego, La Jolla, CA 92093-0411, U.S.A.

(Received 20 June 1995; in revised form 18 September 1995)

Abstract—An experimental investigation of the "Bauschinger effect" in materials under dynamic loading conditions is presented. In this study, a tension split Hopkinson bar with a momentum trap is used to subject a tensile specimen to a single high strain-rate tension pulse of known magnitude and duration. The uniformly deformed gauge length of the tension specimen is then sectioned and loaded in a compression split Hopkinson bar with a momentum trap, at essentially the same strain rate as that of the initial tension test. Comparison is made between these high strain rate Bauschinger experiments and similar tests carried out under quasi-static conditions. Two different material microstructures were examined: solid-solution strengthened and precipitation-strengthened alloys. The Bauschinger effect is found to be a function of the initial material microstructure as well as strain rate. *Copyright © 1996 Acta Metallurgica Inc.*

1. INTRODUCTION

When a material is uniaxially loaded in, for example, tension, into the plastic regime, unloaded, and then reloaded in the reverse direction (i.e. in compression), it is sometimes observed that yielding occurs during the reloading, at a stress lower than if the reloading were carried out in the original direction (tension in this example). This direction-dependent yield behavior is known as the Bauschinger Effect [1]. For various metallic materials [2–8], quasi-static stress-reversal experiments have been performed and corresponding theories developed to characterize microstructural factors affecting the Bauschinger effect. Many processes or events of practical importance, such as impact, forming, wire drawing, earthquakes and blast-loading occur at strain rates ranging from $10^2\,s^{-1}$ to greater than $10^4\,s^{-1}$, and important material parameters such as ductility and strength depend on the applied strain rate.

Conventional mechanical test frames are equipped to perform tests at strain rates between 10^{-6} and $1\,s^{-1}$. The effect of a wide variation in strain rate on the Bauschinger effect has yet to be fully explored due to the lack of proper instrumentation. Nemat-Nasser *et al.* [9] have developed a testing method using Hopkinson bars, where a sample is softly recovered after being subjected to a single, well-defined (tension or compression) pulse of predetermined duration and magnitude. These tension and compression Hopkinson bars can be used to characterize the stress–strain response, work hardening behaviors and, as demonstrated here, the Bauschinger effect in materials at high strain rates.

It is well known that some materials show an increase in flow stress with increasing strain rate. In these rate-sensitive materials, the Bauschinger effect may be misinterpreted if the strain rate happens to be smaller in the stress-reversal cycle of the Bauschinger test. Hence, it is essential that the strain rate in the stress-reversal cycle be nominally equal to the forward loading cycle of the Bauschinger test.

The Bauschinger effect is defined as the change in the flow stress upon stress-reversal. To quantify this change, certain parameters, based on the stress–strain curves, have been introduced in the literature [2–4]. These parameters are termed the Bauschinger-effect parameters and are summarized in a review paper by Abel and Muir [4] and modified later by Moan and Embury [6]. The Bauschinger stress parameter, β_σ, as defined by Moan and Embury, is the fraction of the total work hardening arising from the back stress. It has the form

$$\beta_\sigma = \frac{\sigma_b}{\text{total work hdg.}} = \frac{\sigma_f - |\sigma_r|}{2\sigma_f},$$

where σ_b is the back stress, σ_f is the maximum flow stress in the forward direction (initial loading), and σ_r is the yield stress upon reloading in the opposite direction. The smaller the value of β_σ, the smaller the Bauschinger effect. For small strains in the forward direction, the Bauschinger effect is attributed to the development of long-range (kinematic) stresses during the initial plastic deformation [2–8]. It is well known that material microstructures containing obstacles to dislocation motion (such as precipitates, second-phase particles, or twins) show high hardening rates compared to single-phase or solid-solution strengthened alloys. Due to incompatibility at the obstacle–matrix interface, the pile-up of matrix dislocations is observed. This pile-up of dislocations gives rise to long-range internal stresses which oppose the

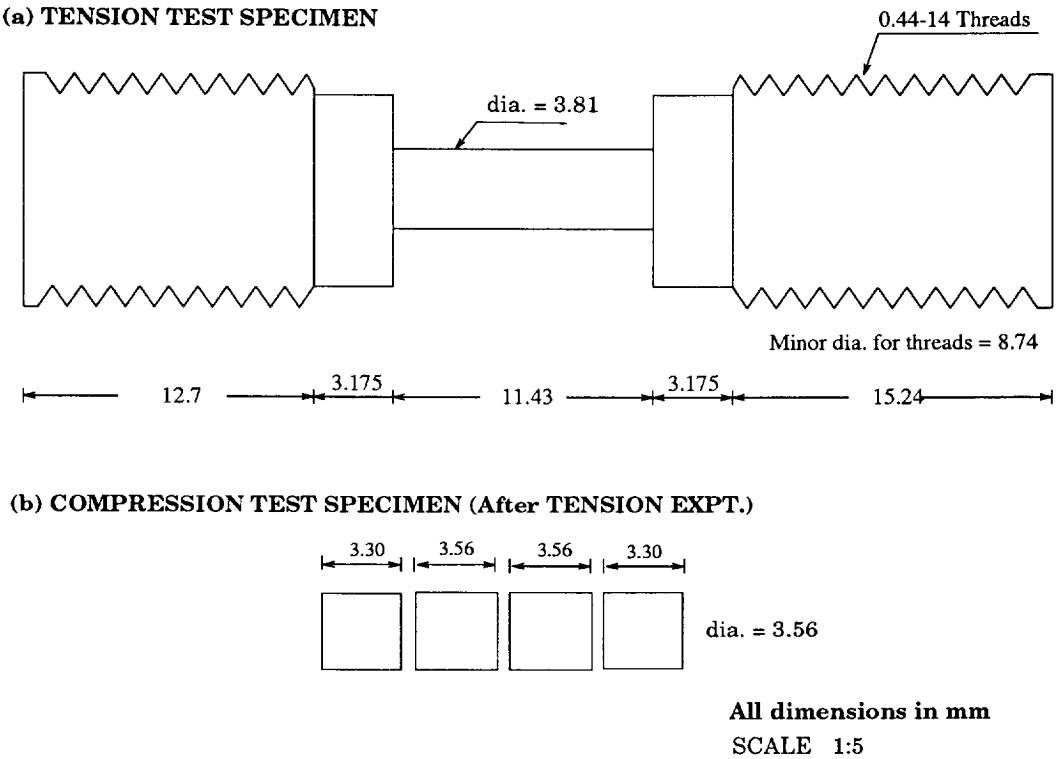

Fig. 1. The sample geometry used for high strain rate Bauschinger experiments: (a) tension specimen and (b) compression specimen.

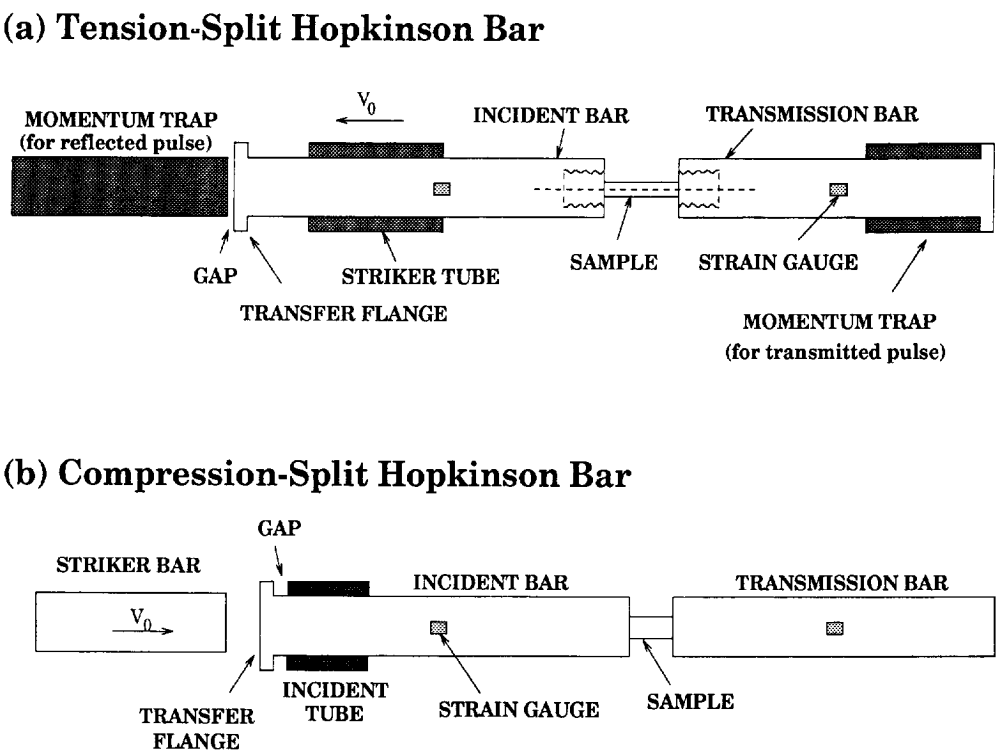

Fig. 2. Schematics of (a) tension and (b) compression split-Hopkinson bars.

further forward plastic deformation. During reverse loading, these long-range internal stresses assist the reverse motion of glide dislocations, lowering the reverse yield stress. It is of interest here to demonstrate an experimental approach to observe the influence of strain rate on the Bauschinger effect. Strain rate is expected to influence the Bauschinger effect, since strain rate affects slip character and hence development of long-range stress.

2. EXPERIMENTAL TECHNIQUE

Modified split Hopkinson bars (SHB) developed by Nemat-Nasser *et al.* [9] were used to measure the stress–strain response of specimens at high strain rates. A tension specimen, as shown in Fig. 1(a), was threaded into the incident and transmitted bars of the tension SHB shown schematically in Fig. 2(a). Wurtz metal was melted into the threaded region to enable a "perfect" match between the sample and the bars. A good fit was obtained when the droplets of wurtz metal were observed to overflow, as the sample was threaded into the bars. A pressurized gas gun drives a striker tube to impact the transfer flange of the incident tension bar; see Fig. 2(a). The transfer flange end of the incident bar is separated from the momentum-trap bar by a prescribed gap such that once the entire tension pulse is transmitted to the incident bar, the gap is essentially closed. The tensile pulse travels towards the specimen, where a part of this pulse is transmitted into the transmission bar through the sample, and the remaining part is reflected as compressive pulse back into the incident bar. This reflected compression pulse travels into the momentum-trap bar, where it is reflected from the rear end of the momentum trap as tension. When this tension pulse reaches the momentum-trap bar–transfer flange interface, it unloads the momentum-trap bar, thus capturing the entire pulse. The transmitted tension pulse is reflected as a compression pulse from the free end of the transmission bar. This compression pulse loads an impedance-matched transmission tube which is in contact with another transfer flange placed at the free end of the transmission bar. This compression pulse is reflected back as a tension pulse from the free end of the transmission tube and is

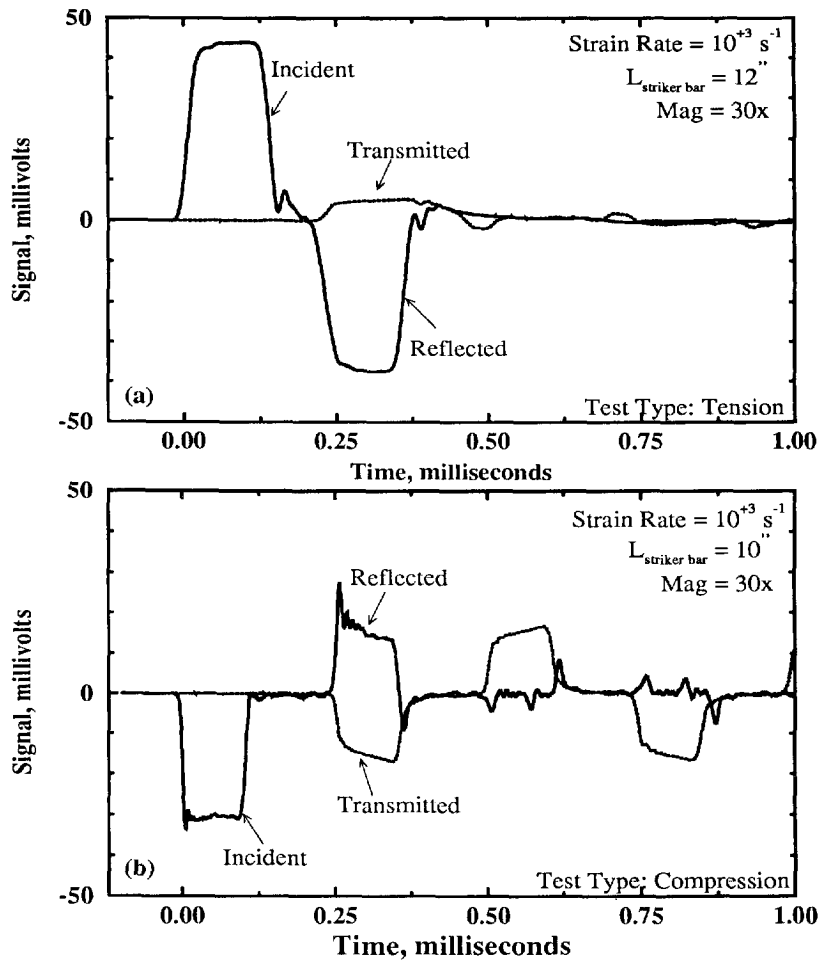

Fig. 3. Typical incident, reflected and transmitted pulse recordings of (a) tension and (b) compression SHB experiments. The reflected and transmitted pulses in the tension test and reflected pulses in the compression test are captured by the respective momentum traps.

trapped by the tube. This ensures that the sample experiences only a single tensile pulse.

Typical pulses, measured by strain gauges which are placed at the centers of the incident and transmission bars, are shown in Fig. 3(a). Examination of these pulses confirmed that the sample was subjected to a single tensile pulse. For tensile reload experiments, the sample was subjected to another tensile pulse of the same magnitude and duration, in order to determine if the reload yield stress in tension was the same as the maximum stress level achieved during the first tensile loading cycle.

In the dynamic Bauschinger test, after the sample was subjected to a single tension pulse, its gauge section was electric discharge machined into four pieces, as shown in Fig. 1(b). The central two pieces were used for dynamic compression tests, using the compression SHB; see Fig. 2(b). In this test the flat ends of the cylindrical sample were lubricated by a thin layer of oil-based molybdenum grease, and the sample was then sandwiched between the incident and transmission compression bars.

In the compression SHB, the striker bar propelled by the gas gun impacts the transfer flange end of the incident bar; see Fig. 2(b). The transfer flange end of the incident bar is separated from the incident tube by a prescribed gap such that once the entire compression pulse is transferred to the incident bar, the gap is essentially closed. Similar to the tension-SHB, the compression pulse which reflects off the sample–incident bar interface as tension, is trapped by an incident tube. The result is illustrated in the pulse recordings of Fig. 3(b). The transmitted compressive pulse is reflected from the rear end of the

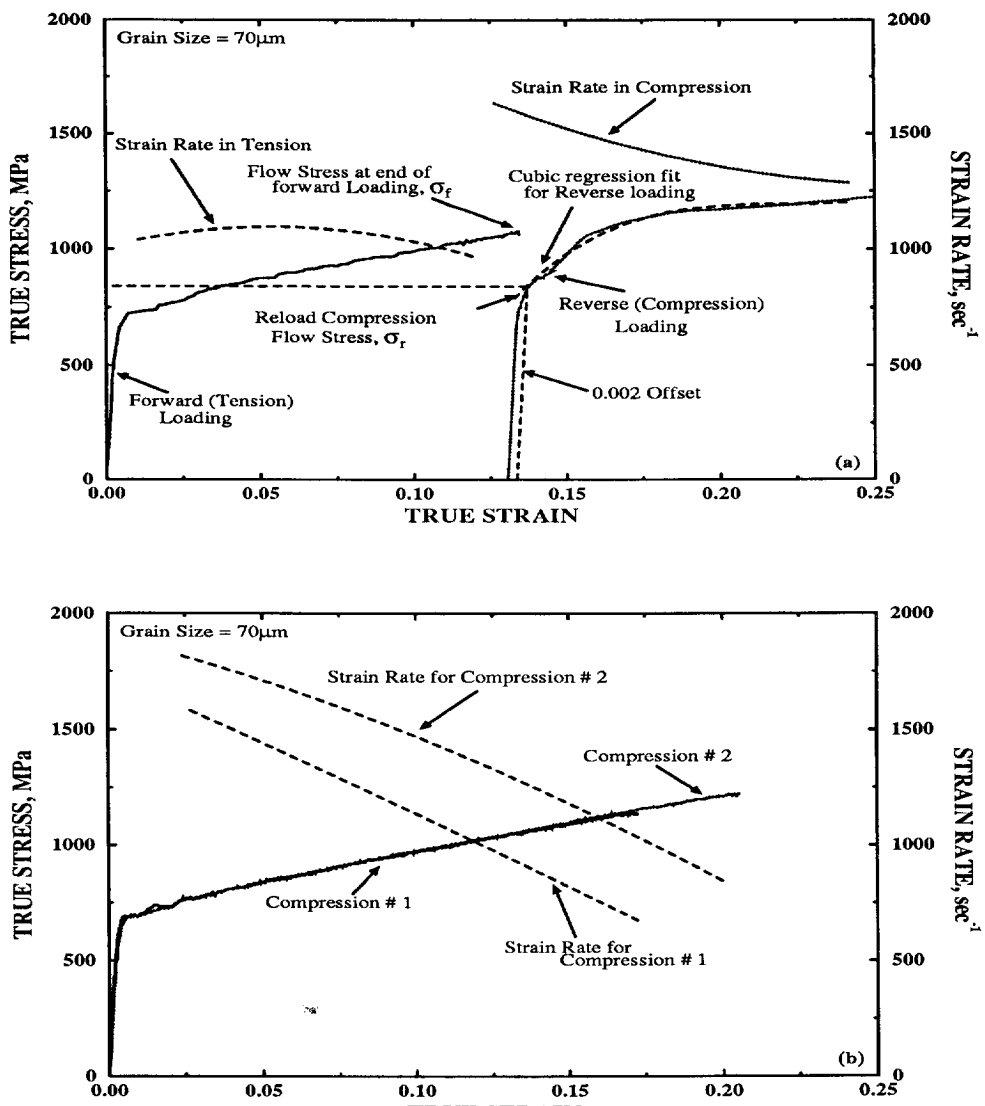

Fig. 4. Typical true stress and strain rate versus true strain plots for the as-received 230^{TM} alloy tested in (a) Bauschinger and (b) compression SHB cycles. The average strain rates in tension and compression cycles of the Bauschinger experiment showed a difference of 300 s^{-1}. Part (b) demonstrates that there is no change in flow stress of the material with a small variation in the strain rate.

transmission bar as a tension pulse which does not affect the compression sample, since this sample is merely sandwiched between the bars and not affixed to either bar. A typical transmitted pulse recording is shown in Fig. 3(b) which gives the stress history of the tested sample. After the completion of the compression test, the sample was safely recovered for further analysis.

For a successful Bauschinger test, one must confirm that the strain rates achieved during the tensile loading and compressive loading are nominally the same. The nominal strain rate and stress in the sample for SHB tests are given by [10]

$$\frac{d\epsilon}{dt}(t) = \frac{2C_b}{L_0}\epsilon_R(t), \text{ and } \sigma(t) = \frac{E_b A_b}{A_0}\epsilon_T(t), \quad (1)$$

respectively. Here, C_b is the sound speed of the bars (4978.4 m/s), E_b is the common Young modulus of the bars (200 GPa), A_b is the common cross-sectional area of the bars, L_0 and A_0 are the initial length and cross-sectional area of the sample, and $\epsilon_R(t)$ and $\epsilon_T(t)$ are the reflected and transmitted strains of the bars measured by the strain gauges as a function of time. The compression SHB with momentum trap was used to subject a sample to a single compression pulse at a desired strain rate of $1200\ s^{-1}$ (same as that of the tension test). To compute the desired strain rate in the compression portion of the dynamic Bauschinger test, a few simplifying assumptions can be made. A flow stress for the sample is assumed to be the maximum flow stress reached in the previous (tensile) loading, allowing the approximate reflected and transmitted strains in the bars to be computed using the above relations. The total incident strain, $\epsilon_I(t)$, in the bar is the algebraic sum of the reflected and transmitted strains in the bar. Assuming that the total kinetic energy of the striker bar goes into producing strain in the incident bar and particle acceleration, one can compute an approximate impact velocity of the striker bar given by

$$\text{velocity of the strike bar}(t) = 2C_b\epsilon_I(t).$$

Typical incident, reflected and transmitted pulse recordings of the tension and compression tests are depicted in Fig. 3. The strain rate, strain and stress as functions of time for the tension and compression SHB are computed from the above relations and used to plot stress versus strain and strain rate versus strain, shown in Fig. 4(a). The average strain rate in tension and compression tests were approximately 1100 and $1450\ s^{-1}$, respectively. Although these strain rates are not identical, they only differ by 30%. In general, materials only exhibit strain rate sensitivity when the strain rate is varied by at least one order of magnitude. With a 30% increase in strain rate, the Bauschinger effect would be slightly reduced for an extremely rate-sensitive material. To illustrate the effect of strain rate on the flow stress of the 230 alloy, two compression tests were performed at different strain rates, as shown in Fig. 4(b). This plot clearly indicates that there is no change in the flow stress of this material with a small variation in a strain rate of $\sim 300\ s^{-1}$ at a nominal strain rate of $1100\ s^{-1}$. Hence, a small increase in the strain rate of the stress-reversal (compression) test, following the forward (tension) test will not affect the flow properties of this material, or alter the observation of a Bauschinger effect.

A universal servohydraulic testing machine (Instron 3200™) was used to study the quasi-static reload tension and stress-reversal responses. Tension specimens with a length to diameter ratio of 5:1 were used to perform displacement-controlled tests. Two tension samples were uniaxially loaded at a strain rate of $10^{-3}\ s^{-1}$ to a true strain of 0.10. One of these samples was reloaded in tension at the same strain rate, to an additional strain of 0.10. The gauge section of the other sample was electric discharge machined to a cylindrical geometry, and then tested in compression using a displacement-controlled mode. The nominal strain rates in the quasi-static tension and compression tests were the same.

The dynamic Bauschinger effect was examined for two materials: nickel-based HAYNES® 230™ alloy and Al-2024 alloy. Figure 5 shows optical micrographs of the as-received 230 alloy and the over-aged Al-2024 alloy. The as-received 230 alloy is a solid-solution strengthened material with annealing twins and large M_6C carbides. In contrast, the Al-2024 alloy was heat treated to an over-aged condition for 1 h at 400°C to precipitate the incoherent θ-phase throughout the grains. In addition, the as-received 230 alloy was heat treated at 760°C for 24 h to precipitate fine, chromium-rich $M_{23}C_6$ carbides (not resolved by optical microscopy). This precipitation-strengthened 230 alloy exhibited an optical microstructure similar to that of the as-received alloy. These two different microstructures of 230 alloy, as-received (solid-solution strengthened) and precipitation strengthened, along with the over-aged Al-2024 alloy were used to investigate the strain rate dependent Bauschinger effect.

The Bauschinger stress parameter, β_σ, was used as a measure of the Bauschinger effect. For the computation of this parameter, several variables were defined through the forward and reverse stress–strain response of the material. The deviation from a linear stress–strain curve in the forward loading (tension) is defined to be the yield point, σ_y. Beyond the yield point, the sample exhibited plastic deformation to a peak true stress of σ_f, where it is then unloaded to zero stress. The material is then reloaded in the opposite direction (compression) at essentially the same strain rate as the forward loading.

In quasi-static reload–compression tests, stress–strain curves with protracted elastic–plastic transitions are obtained. As shown in Fig. 6(a), the elastic portion of the reload–compression curve for the precipitation-strengthened 230 alloy is different from the elastic portion of the reload–tension curve. As such, it is difficult to select a particular value for the

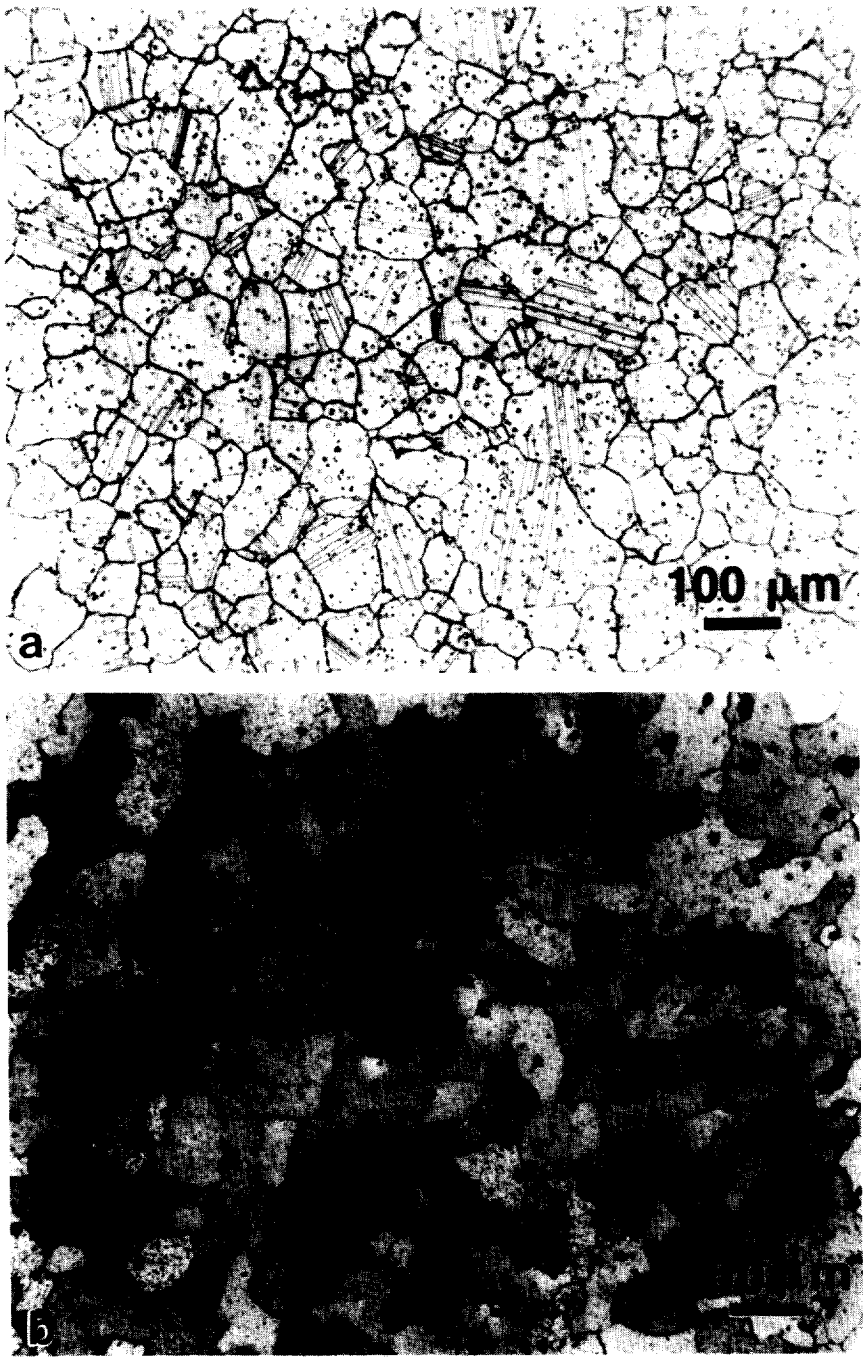

Fig. 5. Optical micrograph of (a) as-received 230 alloy and (b) over-aged Al-2024 alloy.

yield stress in reverse loading. Depending on the flow characteristics of each material, a different criterion is used in the literature to determine the offset yield stress in the reverse direction (see Stout and Rollet [8]). We use a traditional technique to determine the yield stress in the reverse quasi-static loading. In this technique, the stress corresponding to the reverse offset strain of 0.002 is used as a measure of the reverse yield stress, i.e. σ_r.

When these samples are reloaded in the opposite direction at high strain rates, a plateau in the measured flow curve is observed for the initial values of reverse plastic strain; see Figs 4(a) and 6(b). Beyond the plateau region, the sample work hardens at a fairly constant rate after showing a jump in the flow stress value (at approximately 0.02 reverse plastic strain). While this material displays a clear Bauschinger effect, the magnitude of the Bauschinger stress depends largely on the definition of the reverse yield point.

If the deviation from linearity in the stress–strain curve occurs after a uniform stress state is attained

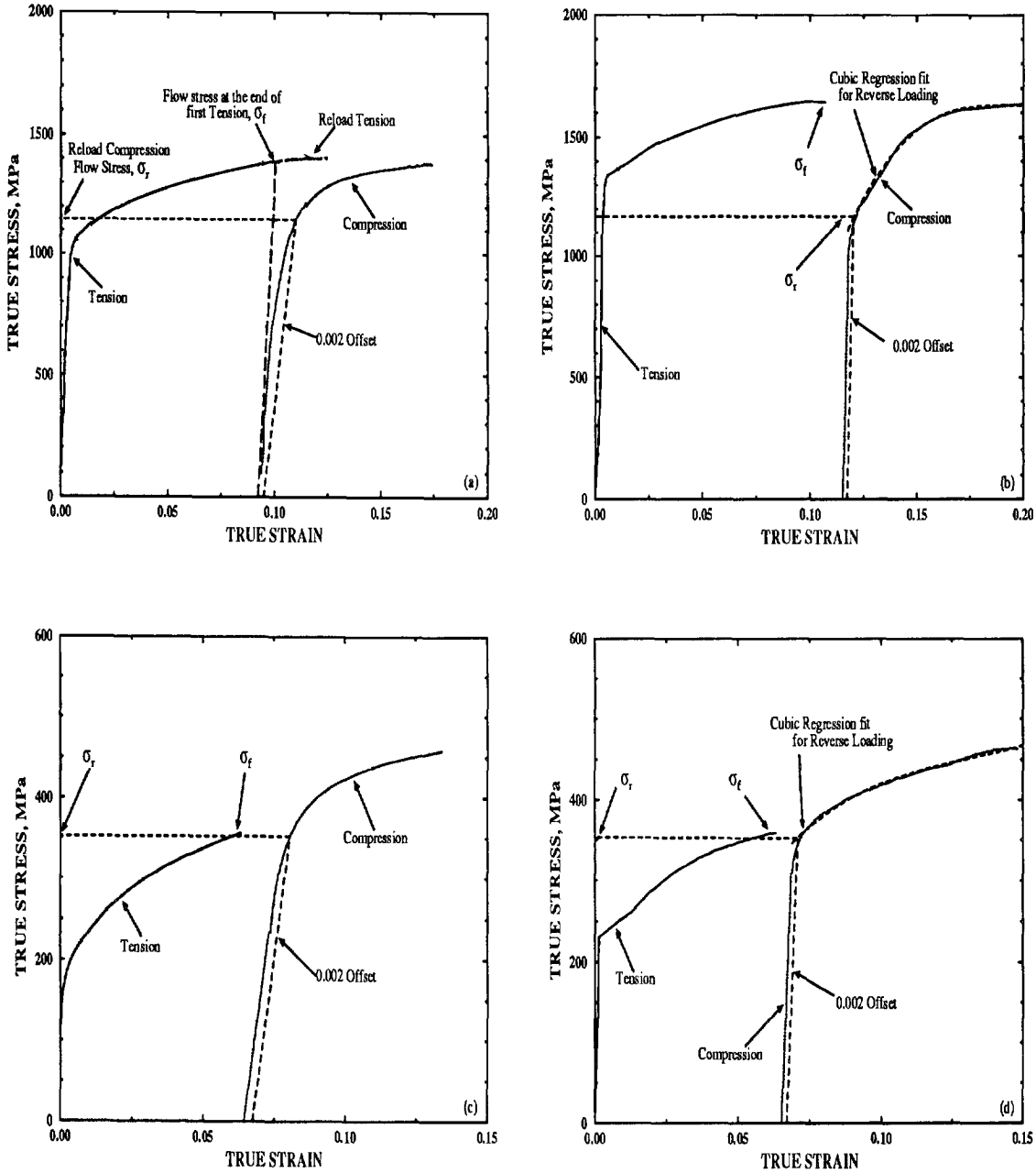

Fig. 6. Bauschinger tests for (a, b) precipitation-strengthened 230™ alloy and (c, d) Al-2024 alloy at different strain rates. Parts (a) and (c) were conducted at a strain rate of $10^{-3}\,s^{-1}$, and (b) and (d) were conducted at a strain rate of $10^{3}\,s^{-1}$. The Bauschinger effect was only observed in the 230™ alloy: (a) and (b).

over the length of the sample, then the corresponding stress value may be regarded as the reverse yield stress. Since the uniaxial elastic wave speed in the sample is 5750 m/s, the stress in a compression sample of 3.56 mm length becomes essentially uniform in about 4 μs [Fig. 7(a)] for the linearly increasing incident compression pulse. The deviation from linearity in the stress–strain curve of the sample is seen to occur at about 10 μs after the incident pulse reaches the sample. The stress in the sample has been uniform for about 6 μs at that instant. The plateau in the stress–strain curve observed after this yield point, appears to be due to Pochhammer–Chree oscillations in the data which are recorded at the center of the bars away from the specimen. In the present case, there is a rather large initial overshoot in the reflected pulse; see Fig. 7(b). This leads to an overestimation of the corresponding plastic strain increment which results in producing the observed plateau. Hence, the observed plateau in the stress–strain curve cannot be used as a material response.

A conservative method to estimate the reverse yield stress at high strain rates has been employed here. A cubic regression fit is used for flow-stress

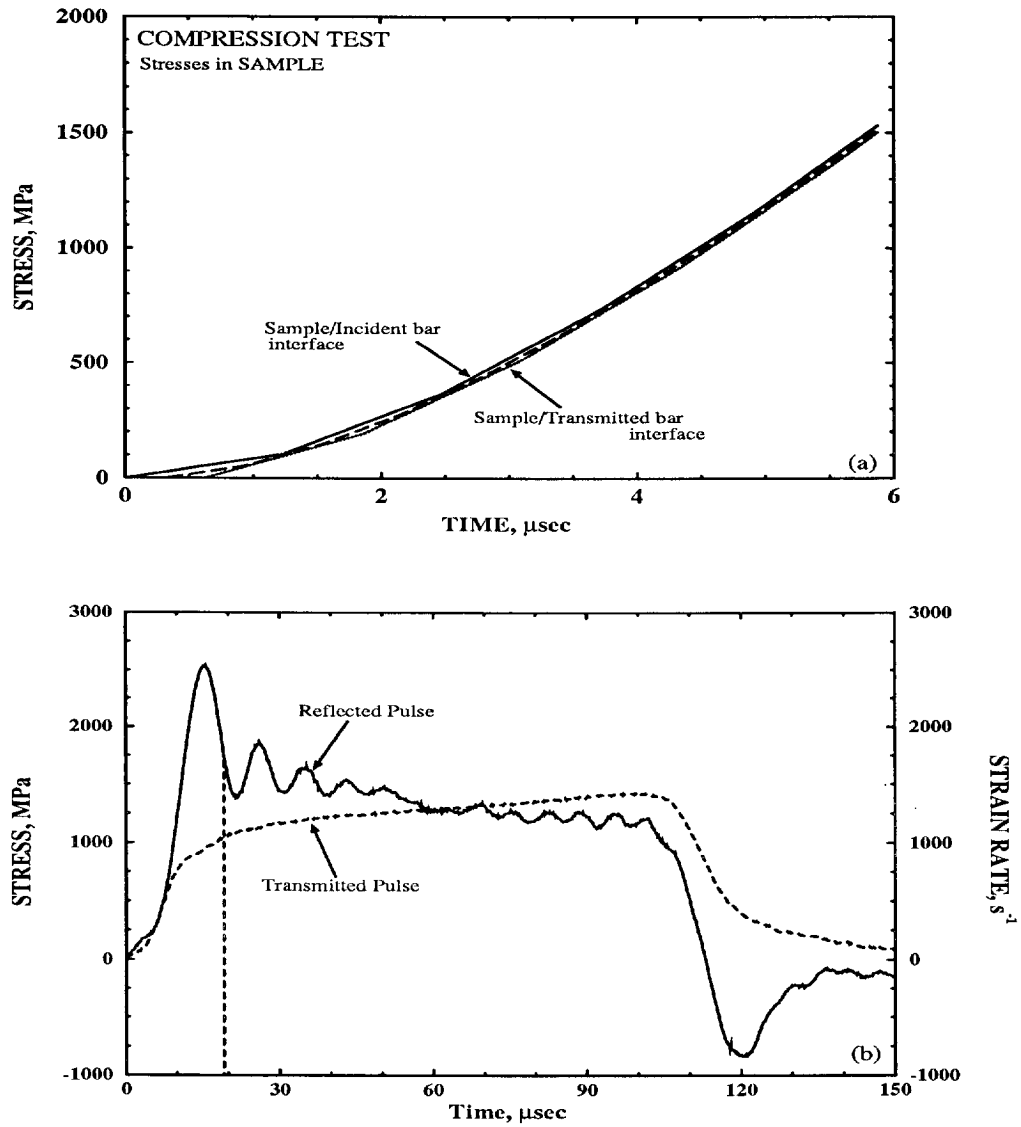

Fig. 7. (a) Computed stress in the sample as a function of time from one-dimensional analysis. (b) Dispersion corrected strain rate (reflected pulse) and stress (transmitted pulse) as a function of time showing large oscillations in the strain-rate versus time plot.

data excluding the plateau region, and then back-extrapolated to the beginning of the reverse flow curve, as shown in Fig. 4(a). Once again, for consistency in the definition, the reverse yield stress value is defined by the 0.002-offset reverse strain (850 MPa in this case), used for the computation of the Bauschinger effect. Note that the reverse yield stress value is higher than the stress level at which the stress–strain curve deviates from linearity and will result in underestimating the Bauschinger effect. From one-dimensional wave computations, at these stress levels the sample is deforming uniformly, and hence, a 0.002-offset reverse strain is a reasonable measure of the reverse yield stress. A cubic regression fit for data beyond 0.02 plastic strain is also back-extrapolated to the beginning of the reload–tension curves. Following this calculation, the reload–tension flow curves are plotted along with the elastic portion of the reload–tension data.

3. RESULTS

The effects of reloading and stress-reversal cycles on the precipitation-strengthened 230 alloy and over-aged Al-2024 alloy at two different strain rates are shown in Fig. 6. The tension and compression curves illustrate the forward and reverse loading cycles of the Bauschinger experiments, respectively. The uniaxial reload–tension response of the samples is also presented. Figures 6(a) and 6(c) depict the quasi-static Bauschinger experiments for the 230 alloy and Al-2024 alloy, respectively. At a strain rate of $10^{-3}\,s^{-1}$, the precipitation-strengthened 230 alloy yielded at 1025 MPa in tension and showed a high rate of hardening. The sample was unloaded after approximately 0.09 strain from a peak stress of 1390 MPa. Upon reloading in tension, the sample failed at a true stress level of 1400 MPa and a true

strain of 0.14. Another tension sample was loaded at a similar strain rate to a true plastic strain of 0.093. The forward loading behavior of this sample, shown in Fig. 6(a), indicates that the sample was unloaded from a peak true stress of 1390 MPa (σ_f). The gauge region of the sample was then sectioned and uniaxially compressed (independently) at the same strain rate of $10^{-3}\,s^{-1}$. A protracted elastic–plastic transition, typical of the true stress–true strain behavior of these samples in uniaxial compression, is depicted in Fig. 6(a). The precipitation-strengthened 230 alloy was found to yield at 1135 MPa (σ_r) upon stress-reversal, and hardened to a true stress of 1380 MPa at a true strain of 0.174. This drop in the flow stress from 1390 to 1135 MPa is characteristic of the Bauschinger effect. At similar strain rates, the over-aged Al-2024 alloy exhibited relatively little work hardening (compared to the 230 alloy) after yielding at 200 MPa. The sample was strained in tension to a peak stress of 350 MPa and unloaded with a residual strain of approximately 0.08. Specimens cut from the gauge section and loaded in compression at a strain rate of $10^{-3}\,s^{-1}$ showed a typical protracted elastic–plastic transition. Upon stress-reversal, the over-aged Al-2024 alloy was found to yield at 350 MPa (σ_r). Hence, under quasi-static loading, the over-aged Al-2024 did not show a Bauschinger effect, in contrast to the Bauschinger effect observed in the precipitation-strengthened 230 alloy.

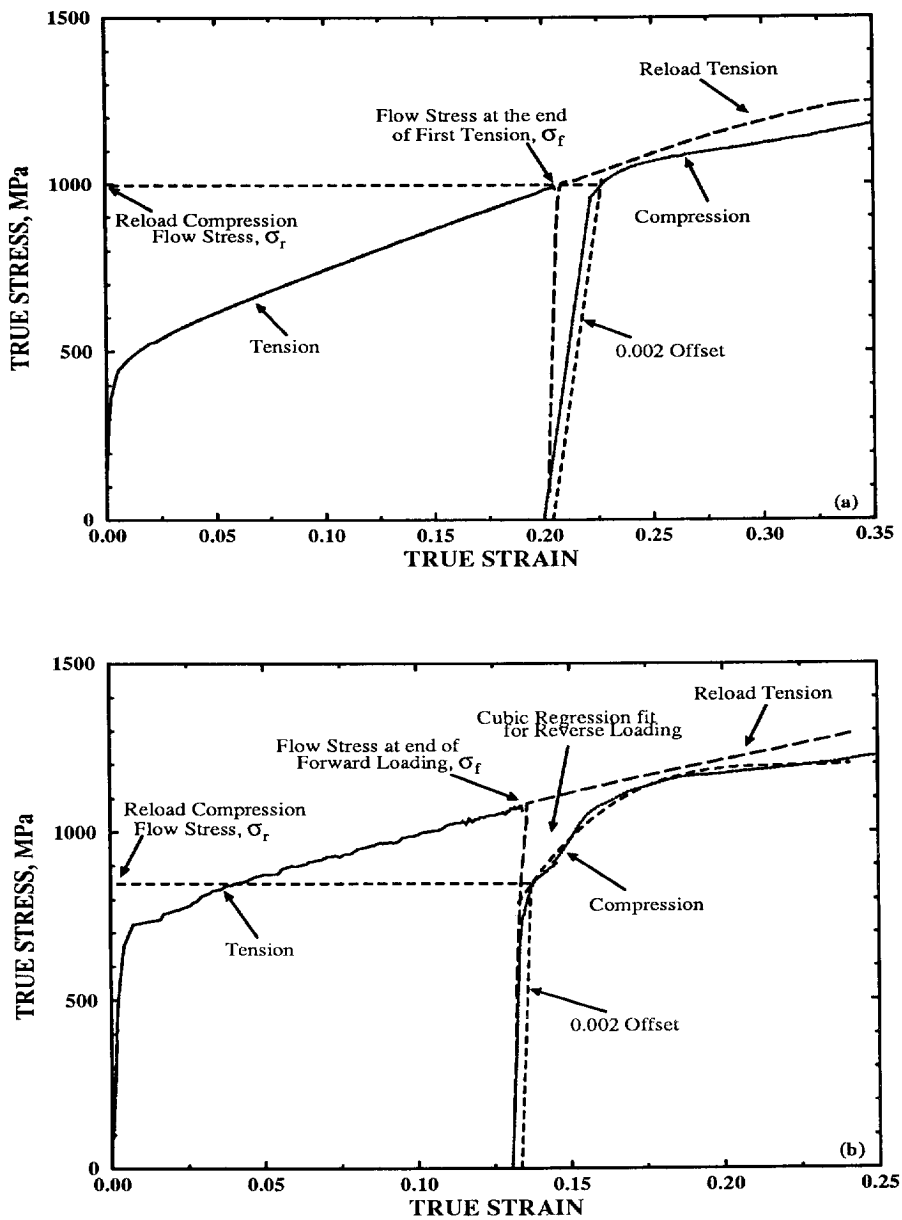

Fig. 8. Bauschinger test for as-received 230™ alloy at different strain rates (a) $10^{-3}\,s^{-1}$ and (b) $10^{3}\,s^{-1}$. The Bauschinger effect was only observed at high strain rate, (b).

High strain-rate reload tension and stress-reversal experiments are depicted through stress–strain curves of Figs 6(b) and 6(d) for the precipitation-strengthened 230 and over-aged Al-2024 alloys, respectively. Two tension samples of each material were loaded with a single tension pulse as shown in Fig. 3(a). This tensile pulse produced a nominal strain rate of $10^3\ s^{-1}$ in the samples. At this strain rate, the 230 alloy yielded at 1350 MPa, and exhibited a high rate of hardening to a peak true stress of 1600 MPa (σ_f). The sample was completely unloaded from this peak stress level with a residual plastic strain of 0.113. One sample was reloaded with the same incident tension pulse (as shown in Fig. 3) and failed during the initial portion of the reloading. The gauge section of the other sample, which had been subjected to a single tension pulse, was cut into four parts and the two central pieces were each loaded with a compression pulse of the magnitude and duration shown in Fig. 3(b). As shown in Fig. 6(b), the sample compressed at a strain rate of $10^3\ s^{-1}$ was observed to flow at 1170 MPa (σ_r), a drop of 430 MPa from the peak stress value ($\sigma_f = 1600$ MPa) reached in the forward loading (tension) cycle. Thus, the precipitation-strengthened 230 alloy exhibited both a quasi-static and a dynamic Bauschinger effect. In contrast, the over-aged Al-2024 alloy did not show a dynamic Bauschinger effect. This is illustrated by the curves of Fig. 6(d) for over-aged Al-2024 alloy which does not show a drop in the flow stress upon stress-reversal (i.e. $\sigma_f = \sigma_r$).

The effect of the strain rate on the reload and stress-reversal tests of the as-received 230 alloy are shown in Fig. 8. Under quasi-static loading, Fig. 8(a), the as-received 230 alloy yields at 460 MPa and fails at 1210 MPa, when loaded monotonically in tension. Another sample was loaded in tension to a peak stress of 990 MPa (σ_f), unloaded, and reloaded in the opposite direction (compression). This sample showed no drop in the flow stress (with respect to σ_f), as depicted in Fig. 8. A similar set of experiments performed at a high strain rate on the as-received 230 alloy is illustrated through the curves of Fig. 8(b). This sample exhibited a dynamic Bauschinger effect with a drop in the flow stress of 240 MPa upon stress-reversal. As such, the Bauschinger effect is strongly affected by both the strain rate and the microstructure of the material.

4. DISCUSSION

The over-aged Al-2024 alloy did not exhibit a Bauschinger effect at either strain rate. It appears that the large spacing between precipitates of over-aged Al-2024 alloy, resulted in low overall long-range stresses which did not contribute to lowering the flow stress upon stress-reversal. In addition, changes in strain rate from 10^{-3} to $10^3\ s^{-1}$ do not appear to be sufficient to alter slip character in Al-2024 alloy from wavy to planar, which may promote a Bauschinger effect.

The as-received (i.e. solid-solution strengthened) 230 alloy exhibited only a dynamic Bauschinger effect, with a Bauschinger stress parameter of 0.11. In contrast, the flow stress upon stress-reversal of the precipitation-strengthened 230 alloy dropped by 255 MPa at low strain rate and by 315 MPa at high strain rate. A Bauschinger stress parameter of 0.135 was calculated for the high strain-rate experiment, and a value of 0.092 for the quasi-static experiment. This parameter is a measure of the average elastic stresses developed during the forward (tension) loading. It is postulated here, that the more pronounced Bauschinger effect observed at high strain rate in both conditions of 230 alloy, is due to the greater propensity for planar slip with increasing strain rate, and will be investigated further via transmission electron microscopy.

Several important strain rate aspects of the Bauschinger effect observed in metallic materials can now be examined through the use of dynamic Bauschinger experiments described above, including: changes in slip mode accompanying strain rate changes; increased dislocation activation due to elevated flow stresses at higher strain rates, particularly important in b.c.c. materials; and increased hardening rates at high strain rates in f.c.c. materials. Each of these effects has the propensity to produce a Bauschinger effect in materials which may not exhibit a Bauschinger effect at low strain rates, or potentially enhance the magnitude of the effect in materials which usually exhibit a Bauschinger effect at low strain rate. In other words, those deformation and strengthening mechanisms which are thermally-activated processes can be influenced by increasing strain rates. As such, any thermally-activated processes which are sufficiently strain-rate sensitive, may produce a Bauschinger effect in a dynamic Bauschinger experiment.

5. CONCLUSION

A new experimental technique has been presented to demonstrate the Bauschinger effect in materials under dynamic loading conditions. Modified split-Hopkinson bars developed by Nemat-Nasser *et al.* [9] were used to study the dynamic Bauschinger effect in two materials: HAYNES® 230™ alloy and Al-2024 alloy. In this study, tensile specimens were softly recovered after having been subjected to a single tension pulse of known magnitude and duration. The uniformly deformed gauge section of the tension sample was then sectioned and reloaded in compression, using essentially the same strain rate as in the initial tensile loading. Quasi-static reload–tension and stress-reversal compression experiments were performed for comparison to examine the effect of strain rate on the Bauschinger effect. The over-aged Al-2024 alloy did not exhibit a Bauschinger effect at

either low or high strain rates. The as-received 230 alloy did not exhibit a quasi-static Bauschinger effect, but did exhibit a pronounced Bauschinger effect under high strain rate conditions. The magnitude of the Bauschinger effect was observed to increase with increasing strain rate for the precipitation-strengthened 230 alloy which exhibited quasi-static and dynamic Bauschinger effect.

Acknowledgements—This work has been supported by the U.S. Army Research Office under contracts No. DAAL-03-86-K-0169 and No. DAAL-03-92-G-0108, with the University of California, San Diego. The authors wish to thank Professor M. M. Rashid, Dr G. T. Gray III and Mr Jon Isaacs for useful discussions. Superalloy materials were gratefully donated by HAYNES International, Kokomo, IN.

REFERENCES

1. J. Bauschinger, *Civilingenieur* **27,** 289 (1881).
2. R. L. Woolley, *Phil. Mag.* **44,** 597 (1953).
3. D. V. Wilson, *Acta metall.* **13,** 807 (1964).
4. A. Abel and H. Muir, *Phil. Mag.* **26,** 489(1972).
5. R. E. Stoltz and R. M. Pelloux, *Scripta metall.* **8,** 269 (1974).
6. G. D. Moan and J. D. Embury, *Acta metall.* **27,** 903 (1979).
7. U. K. Hidayetoglu, P. N. Pica and W. L. Haworth, *Mater. Sci. Engng* **73,** 65 (1985).
8. M. G. Stout and A. D. Rollet, *Metall. Trans. A* **21A,** 3201 (1990).
9. S. Nemat-Nasser, J. B. Isaacs and J. E. Starrett, *Proc. R. Soc. Lond. A* **435,** 371 (1991).
10. P. S. Follansbee, in *Mechanical Testing, Metals Handbook* (edited by A. Committee), Vol. 8, pp. 190–207. ASM, OH, 44073, ninth edition (1985).